

Fully Inkjet-printed Multi-layer Tunable Origami FSS Structures with Integrated Thermal Actuation Mechanism

Syed Abdullah Nauroze, Manos M. Tentzeris
 School of Electrical and Computer Engineering
 Georgia Institute of Technology
 Atlanta, Georgia 30332-0250

Abstract—A first-of-its-kind design methodology to realize origami-inspired multi-layer frequency selective surfaces (FSS) with a thermally actuated smart shape-shifting spacer layer is presented. The spacer not only features low dielectric losses but can also change its shape to maintain optimum inter-layer distances as the Miura-FSS structure is folded to preserve desired frequency response. It also introduces unprecedented high mechanical strength making it suitable for wide range of applications. The proposed structure features twice as broad bandwidth as compared to single layer Miura-FSS and an excellent angle of incidence rejection.

Keywords—Multilayer frequency selective surface, origami, Miura, tunable filters, inkjet-printing

I. INTRODUCTION

Frequency Selective Surfaces (FSSs) are spatial filters that reflect, transmit or absorb band of incident electromagnetic waves and typically consists of a 2D or 3D periodic array of resonant elements on a thin substrate. The frequency response of an FSS is primarily determined by the size, shape and type of the resonant element along with their inter-element distances. These structures have found many applications including radomes, reflectors, transmitarrays and reducing antenna radar cross section [1], [2]. Traditional FSS structures are unable to change their frequency response which limits their use in real-life applications. One of the most popular tuning mechanism for these structures is integration of electronic components such as varactors with the resonant elements. However, this approach is laborious, expensive, requires high operational voltages and makes the overall frequency response non-linear as the structure size increases. In contrast, mechanical tuning mechanisms features superior power handing capability, quality factor, linearity and wide-band (continuous range) tunability. However, their bulky size, heavy weight and low switching/tuning speed has restricted their use in modern communication systems.

Recently, origami-inspired single-layer Miura FSS structures have been proposed [3]–[5] that realize tunability by either changing electrical length or inter-element coupling. However, single layer Miura-FSS (SLM-FSS) structures have limited bandwidth, lower mechanical strength and tunability range which limits their use in practical applications. Moreover, a single layer Miura structures with non-rigid facets tend to curl up the whole structure when folded, thereby changing frequency response of the FSS structure [6]. Also previously presented work used paper-based substrate that requires mechanical actuation to fold the Miura structure

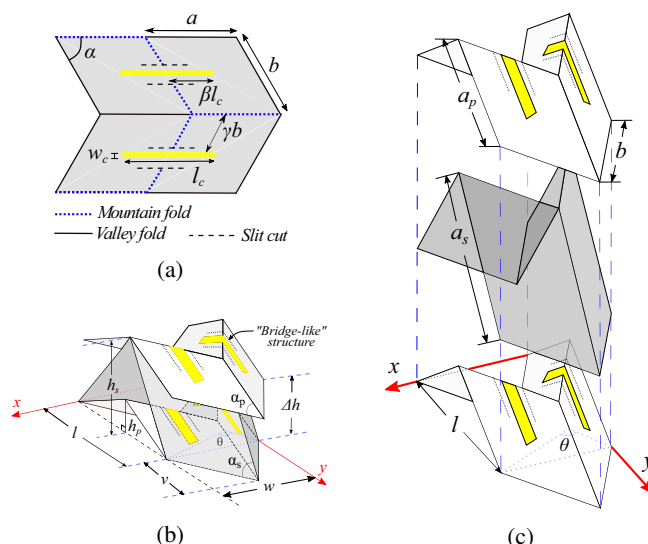


Fig. 1. (a) Unit cell of a SLM-FSS in flat configuration ($\theta = 180^\circ$). Unit cell of MLM-FSS in folded configuration ($\alpha_p = 45^\circ$) (c) exploded view of the MLM-FSS with $b_s = b_p = b = a_p = 20\text{mm}$. $\beta = \gamma = 0.5$, $l_c = 20\text{mm}$ and $w_c = 2\text{mm}$. Top and bottom Miura-FSS use paper substrate while spacer uses polyester film.

which makes it unsuitable for outer-space and biomedical applications where available power is limited. These problems can be mitigated by using multi-layer Miura FSS (MLM-FSS) configurations, however, realization of a shape-reconfigurable spacer layer between the SLM-FSS structures that can change inter-layer distance according to the variation in frequency response of the SLM-FSS is challenging.

This paper introduces a novel approach to realize fully inkjet-printed MLM-FSS structure with a heat sensitive, shape configurable spacer between identical (paper-based) Miura-FSS structures that not only preserves the in-plane kinematics but also facilitate proportional change the inter-layer distance between them as the structure is folded. The Miura-FSS consists of dipole array elements that are inkjet-printed across the foldlines of the Miura structure. The multilayer Miura-FSS configuration drastically increases the mechanical strength of the overall structure making it useful for a wide range of applications. The MLM-FSS is simulated and measured to evaluate its performance with respect to variation in angle of incidence and folding configurations.

II. MULTI-LAYER MIURA-FSS STRUCTURES WITH DIPOLE ELEMENTS

The unit cell of Miura-Ori tessellation consists of four parallelograms (each with length a , b and an internal angle α) connected to each other along the edges to form the foldlines as shown in Fig. 1a. The foldlines either curve up (mountain fold) or curve down (valley fold) as the Miura structure is folded, depicted by change in dihedral angle θ or equivalently lengths w or l that are related to each other by [3]:

$$\begin{aligned} l &= 2a\zeta, & h &= a\zeta \tan \alpha \cos(\theta/2) \\ w &= 2b\xi, & v &= b(1 - \xi^2)^{1/2} \end{aligned} \quad (1)$$

where,

$$\zeta = \cos \alpha (1 - \xi^2)^{-1/2}, \quad \xi = \sin \alpha \sin(\theta/2) \quad (2)$$

SLM-FSS is realized by inkjet-printing dipoles across the mountain foldlines of Miura-Ori tessellation as shown in Fig. 1a. Since the dipoles are inkjet-printed on the mountain folds, the electrical length and inter-element distances between the dipoles systematically decreases as θ varies from 180° (flat configuration) to 0° (completely folded configuration) [3] [7]. The electrical length of the dipole decreases with θ due to its shape transformation from a 2D structure to an inverted V-shaped dipole structure, thereby shifting the overall frequency response of the SLM-FSS to higher values. However, they feature 15% frequency tunability and moderate bandwidth (10%) [3] which limits their use in real-life applications. Therefore, tunable MLM-FSS structures with optimum inter-layer distances is required to realize higher-order bandstop frequency response.

Conventional multilayer FSS structures consist of two or more FSSs that are separated by a distance Δh using either special mechanical support or thick dielectric. Since inter-layer distance depicts electromagnetic coupling between the FSS layers, it must also change proportionally with respect to the variation in frequency response of the FSS layers to preserve desired frequency response. This problem is addressed in this paper by using a heat sensitive shape-reconfigurable spacer between two identical cellulose-paper based SLM-FSS structures to form the MLM-FSS as shown in Fig. 1b. The heat sensitive material consists of a rigid $90 \mu\text{m}$ thick polyester based film ($\epsilon_r = 2.92$, $\tan \delta = 0.0088$ at 8GHz) which softens and unfolds when heated beyond 50°C as shown in Fig. 2. It should be noted here that single layer of polyester film expands more than the MLM-FSS at relatively moderate temperature because latter has paper based SLM-FSS on both sides of the spacer reducing effective surface temperature.

In order to maintain the in-plane kinematics of the proposed MLM-FSS structure, all Miura layers must have same w , l and v values with only one independent dimension h thereby facilitating the inter-layer distance (Δh) to vary proportionally with different folding configurations. These conditions can be met by using following design constraints:

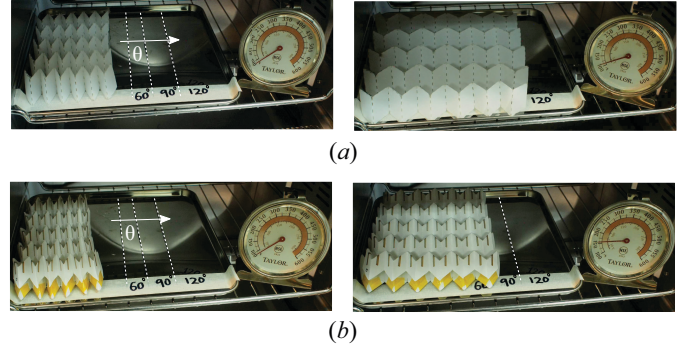


Fig. 2. Thermal actuation of (a) single layer polyester film-based Miura structure (b) MLM-FSS structure. The marking indicates Miura extension for different values of θ

$$a_s = a_p \frac{\cos(\alpha_p)}{\cos(\alpha_s)}, \quad b_s = b_p = b \quad (3)$$

where, the subscripts p and s represents the design parameters of the paper-based and spacer Miura structures respectively. Since the proposed multi-layer Miura-FSS configuration preserves the in-line kinematics of the overall structure, the kinematics of the overall structure can still be completely described by the folding angle θ . The inter-layer distance (Δh) can be calculated by using first calculating h for the two layers using eq. 4 and then taking the difference between them.

The heat sensitive spacer in MLM-FSS facilitates controlled actuation of the overall structure making an attractive candidate for terrestrial, outer-space and electromagnetic cloaking applications where the frequency response can be changed on-demand by simply varying the folding angle (increasing temperature). The Miura geometry also facilitates perfect alignment of multiple FSS layers by simply stacking them along the valley foldlines as shown in Fig. 1b and 1c thereby mitigating alignment errors during assembly. Since the spacer consists of a very thin layer of low loss material, the effects of the dielectric losses can be ignored [1]. Moreover, the proposed MLM-FSS features higher mechanical strength as compared to SLM-FSS despite its low thickness as shown in Fig. 3 making it an attractive candidate for rugged environment and sandwich structures used in aerospace, structural and mechanical engineering applications [8].

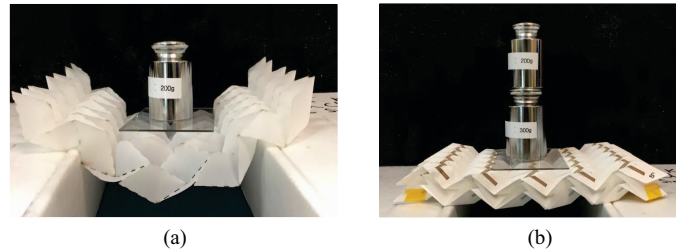


Fig. 3. Structural response of (a) single-layer polyester-based Miura structure (b) MLM-FSS with polyester spacer

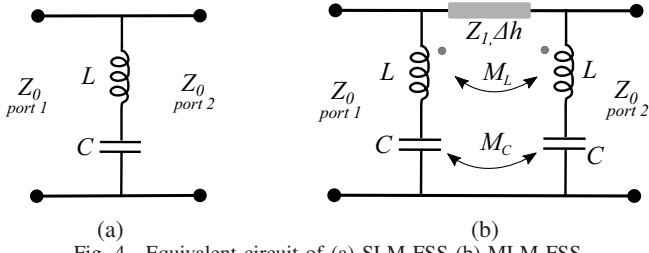


Fig. 4. Equivalent circuit of (a) SLM-FSS (b) MLM-FSS

The electromagnetic behavior of the MLM-FSS can be approximated using equivalent circuit model where each SLM-FSS layer with dipole elements can be represented by a series LC network connected across two ports with intrinsic impedance ($Z_o=377\ \Omega$) as shown in Fig. 4a – a first-order bandstop filter. The corresponding values of the inductance (L) and capacitance (C) are dictated by dipole length and their inter-element distances respectively [1]. Similarly, the equivalent circuit of the proposed MLM-FSS is shown in Fig. 4b where the values of L and C are same as for the SLM-FSS and the spacer is represented by a transmission line whose length (l) depends on thickness of the spacer [9]. The characteristic impedance of the spacer is $Z_l = Z_o/\sqrt{\epsilon_r}$, where ϵ_r & Z_o relative permittivity of spacer & characteristic impedance of free space respectively. However, the dielectric effects of the spacer can be ignored in our case as the effective permittivity of the spacer is almost equal to that of free space (ϵ_o). Hence the equivalent model of the proposed Miura-FSS can be reduced to two series LC network connected across the two ports where the mutual inductance and capacitance between the layers is represented by M_L and M_C respectively. These coupling co-efficients controls the resonant frequency and the bandwidth of the FSS structure [10], [11]. The numerical values of L , C , M_L and M_C can be calculated by procedure outlined in [12] and are related to each other by [1]:

$$\omega_r = \frac{1}{\sqrt{LC}}, \quad L_M = \mu_o\mu_r\Delta h, \quad L_C = \frac{\epsilon_o\epsilon_r\Delta h}{2} \quad (4)$$

where, ω_r is the resonant frequency of the SLM-FSS, while μ_o & μ_r are permeability of free space & relative permeability of the spacer respectively.

The proposed MLM-FSS was fabricated by first realizing two identical SLM-FSS on $110\ \mu m$ thick cellulose paper; then, the dipoles were inkjet-printed across the foldlines using 10 layers of silver nanoparticle (SNP) ink and sintered at $150^\circ C$ for 2hrs to increase conductivity. The resultant dipoles are highly flexible and maintain high conductivity during bending or folding process since the conductive ink is embedded into the substrate due to its hydrophilic nature [3], [13]. The flexibility of the dipoles is further enhanced by cutting slits along the dipoles to realize special “bridge-like” structures that fold dipoles in a smooth curved fashion along the foldlines rather than a sharp edge [3] [7] as the Miura is folded. Similarly, Miura pattern with desired α_s is perforated on the polyster film. Finally, the three Miura structures are folded

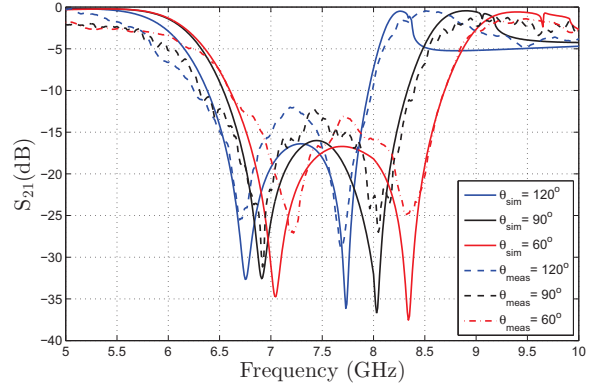


Fig. 5. Frequency response of a MLM-FSS structure ($\alpha_s = 56^\circ$) for different values of folding angle (θ)

manually, stacked (along valley foldlines) and joined together using thermal resistant glue on the mountain folds.

III. SIMULATION AND MEASUREMENT RESULTS

The unit cell of the proposed MLM-FSS was simulated using master/slave boundary conditions in HFSS with Floquet port excitation. The simulated results were then verified by using two broadband horn antennas in line-of-sight to each other with the MLM-FSS in the middle. Specialized 3D printed frames were used to hold the MLM-FSS structure at $\theta=60^\circ, 90^\circ, 120^\circ$. However, these frames would not be required for practical applications as θ can be increased by simple temperature variation.

The simulated and measured insertion loss (S_{21}) of MLM-FSS with respect to different values of α_s is shown in Fig. 6 which clearly indicates that at lower values of α_s , the structure exhibits broadband behavior with two distinct resonances. The lower resonance frequency is result of mutual coupling between the two SLM-FSS layers, while the higher frequency is the resonant frequency of the individual SLM-FSS layers. The inter-layer distance increases with α_s resulting in the shifting the coupling frequency towards the resonant frequency that eventually merge together at $\alpha_s=68^\circ$

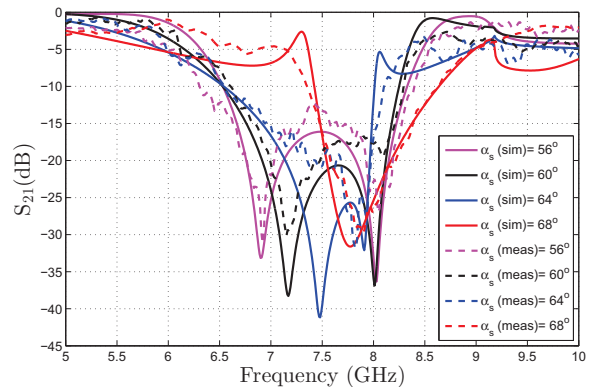


Fig. 6. Frequency response of a MLM-FSS structure ($\theta = 90^\circ$) for different values of internal angle of spacer (α_s)

where $\Delta h \approx 22.5\text{mm} \approx \lambda/2$ – a necessary condition for strong coupling between multilayer FSS structures.

Similarly, it is interesting to note here that not only the frequency response of the proposed MLM-FSS systematically shifts to higher frequency, but its filter response is also preserved with variation in θ as shown in Fig. 5. This clearly shows that the proposed spacer vary the inter-layer distance proportionally with respect to shift in resonant frequency of the two SLM-FSS layers during all folding states. The proposed structure facilitates a bandwidth up to 24% which is more than twice the bandwidth of the equivalent SLM-FSS, however the tunability range is comparable which can be increased by using ripple-Miura FSS [5]. The sudden null in the frequency response indicates onset of the grating lobe which also changes with θ , thereby avoiding any unwanted diffraction effects [1]. Lastly, the proposed MLM-FSS features a very wide-angle angle of incidence (AoI) rejection (upto 75°) without any shift in resonance frequency as shown in Fig. 7. The increase in bandwidth is an inherent feature of the dipole FSS which increases as $1/\cos(\text{AoI})$ for different values of AoI in the H-plane [1].

IV. CONCLUSION

The paper presents a state-of-the-art fully inkjet-printed MLM-FSS structure with dipole resonant elements and an integrated thermally actuated, shape reconfigurable spacer layer that addresses some of the major drawbacks of the previously reported single layer Miura-FSS structures. This includes narrow band frequency response, poor mechanical stability and use of mechanical actuation mechanism which may not be suitable for applications with limited available power for actuation. The smart shape-shifting spacer is the first demonstration of its kind which preserves the in-plane kinematics and proportionally vary the inter-layer distances between multi-layer Miura FSS structures for every folding configuration, thereby maintaining the desired frequency response of the filter. The realized bandwidth of the proposed structure is more than double as compared to SLM-FSS structure and can be varied by simply changing

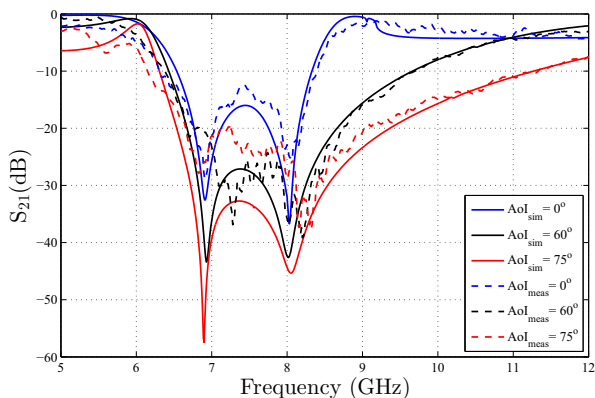


Fig. 7. Frequency response of MLM-FSS ($\theta = 90^\circ$, $\alpha_s = 56^\circ$) for different values of angle of incidence

the dimensions of the spacer layer. It also facilitates perfect alignment of the Miura-FSS structure to mitigate any misalignment errors that may occur during the assembly. A detailed analysis of the MLM-FSS structure with respect to change in folding angle (θ), angle of incidence (AoI) and inter-layer distances is presented in this paper. Moreover, the electromagnetic behavior of the structure is also explained in terms of the equivalent circuit model. The simulation results strongly agrees with the measured results. Moreover, the proposed design truly represents the uniqueness and substantial advantage of additive manufacturing technologies and origami-inspired RF structures since these structures would be impossible to realize using traditional manufacturing technologies. Moreover, the presented design principles can be extended to realize higher-order tunable FSS structures without loss of generality giving the designer the freedom to design custom-based FSS structure suitable for a given application.

REFERENCES

- [1] B. A. Munk, "Frequency selective surfaces theory and design. John Wiley & Sons," 2000.
- [2] T. Wu, *Frequency Selective Surface and Grid Array*, ser. Wiley Series in Microwave and Optical Engineering. Wiley, 1995.
- [3] S. A. Nauroze, L. Novelino, M. M. Tentzeris, and G. H. Paulino, "Inkjet-printed "4d" tunable spatial filters using on-demand foldable surfaces," in *2017 IEEE MTT-S International Microwave Symposium (IMS)*, June 2017, pp. 1575–1578.
- [4] K. Fuchi, J. Tang, B. Crowgey, A. R. Diaz, E. J. Rothwell, and R. O. Ouedraogo, "Origami tunable frequency selective surfaces," *IEEE Antennas and Wireless Propagation Letters*, vol. 11, pp. 473–475, 2012.
- [5] S. A. Nauroze, A. Eid, and M. M. Tentzeris, "n-rim: A paradigm shift in the realization of fully inkjet-printed broadband tunable fss using origami structures," in *2018 IEEE/MTT-S International Microwave Symposium - IMS*, June 2018, pp. 51–54.
- [6] S. A. Nauroze, L. S. Novelino, M. M. Tentzeris, and G. H. Paulino, "Continuous-range tunable multilayer frequency-selective surfaces using origami and inkjet printing," *Proceedings of the National Academy of Sciences*, vol. 115, no. 52, pp. 13 210–13 215, 2018.
- [7] S. A. Nauroze, J. G. Hester, B. K. Tehrani, W. Su, J. Bitto, R. Bahr, J. Kimionis, and M. M. Tentzeris, "Additively manufactured rf components and modules: Toward empowering the birth of cost-efficient dense and ubiquitous iot implementations," *Proceedings of the IEEE*, vol. 105, no. 4, pp. 702–722, April 2017.
- [8] Y. Klett, P. Middendorf, W. Sobek, W. Haase, and M. Heidingsfeld, "Potential of origami-based shell elements as next-generation envelope components," in *2017 IEEE International Conference on Advanced Intelligent Mechatronics (AIM)*, July 2017, pp. 916–920.
- [9] K. Sarabandi and N. Behdad, "A frequency selective surface with miniaturized elements," *IEEE Transactions on Antennas and Propagation*, vol. 55, no. 5, pp. 1239–1245, May 2007.
- [10] X. Hu, X. Zhou, L. Wu, L. Zhou, and W. Yin, "A miniaturized dual-band frequency selective surface (fss) with closed loop and its complementary pattern," *IEEE Antennas and Wireless Propagation Letters*, vol. 8, pp. 1374–1377, 2009.
- [11] A. A. Dewani, S. G. O’Keefe, and D. V. Thiel, "Transmission bandwidth enhancement using lateral displacement in a thin flexible single layer double sided fss," in *2015 International Symposium on Antennas and Propagation (ISAP)*, Nov 2015, pp. 1–4.
- [12] F. Costa, A. Monorchio, and G. Manara, "An overview of equivalent circuit modeling techniques of frequency selective surfaces and metasurfaces," *Appl. Comput. Electromagn. Soc. J.*, vol. 29, no. 12, pp. 960–976, 2014.
- [13] S. A. Nauroze, J. Hester, W. Su, and M. M. Tentzeris, "Inkjet-printed substrate integrated waveguides (siw) with "drill-less" vias on paper substrates," in *Microwave Symposium (IMS), 2016 IEEE MTT-S International*. IEEE, 2016, pp. 1–4.